The Retina of *c-fos*$^{-/-}$ Mice: Electrophysiologic, Morphologic and Biochemical Aspects

Nicole Kueng-Hitz,[1] *Christian Grimm,*[2] *Nicola Lansel,*[1] *Farhad Hafezi,*[2] *Lihua He,*[3] *Donald A. Fox,*[3] *Charlotte E. Remé,*[2] *Günter Niemeyer,*[1] *and Andreas Wenzel*[2]

Purpose. Mice without a functional c-Fos protein (*c-fos*$^{-/-}$ mice) do not exhibit light-induced apoptotic cell death of rods in contrast to their wild-type littermates (*c-fos*$^{+/+}$ mice). To analyze the consequences of the absence of *c-fos* in the retina, we investigated whether the retinas of *c-fos*$^{-/-}$ mice have a reduced capacity to absorb and transduce light compared with *c-fos*$^{+/+}$ mice.

Methods. Retinal function was evaluated in dark-adapted mice by full-field electroretinograms (ERGs) over more than 6 log units of intensity. Retinal morphology was studied by light- and electron microscopy. Arrestin and the heat shock protein 70 (Hsp70) were detected by Western blot analysis. The rhodopsin content and the kinetics of rhodopsin regeneration were determined in retinal extracts.

Results. Although the configuration of the ERGs was comparable in both groups of mice, *c-fos*$^{-/-}$ mice showed a marked variability in all quantitative ERG-measures with lower mean amplitudes, longer latencies, and a 0.9-log-unit lower b-wave sensitivity on average. Morphometry showed that *c-fos*$^{-/-}$ mice have 23% fewer rods on average, whereas the number of cones was comparable among *c-fos*$^{+/+}$ and *c-fos*$^{-/-}$ mice. Arrestin levels appeared slightly reduced in *c-fos*$^{-/-}$ mice when compared with *c-fos*$^{+/+}$ mice, whereas Hsp70 levels were comparable in both genotypes. The kinetics of rhodopsin regeneration were similar, but *c-fos*$^{-/-}$ mice had a 25% lower rhodopsin content on average.

Conclusions. Compared with *c-fos*$^{+/+}$ mice, retinal function in *c-fos*$^{-/-}$ mice is attenuated to a variable but marked degree, which may be, at least in part, related to the reduced number of rods and the reduced rhodopsin content. However, *c-fos* does not appear to be essential for the ability to absorb photons, nor for phototransduction or the function of second-order neurons. The resistance to light-induced apoptosis of photoreceptor cells in *c-fos*$^{-/-}$ mice may result from the acute deficit of *c-fos* in the apoptotic cascade rather than from developmental deficits affecting rod photoreceptor function. (*Invest Ophthalmol Vis Sci.* 2000;41:909–916)

Apoptotic cell death in the retina occurs not only during normal development[1] but also under a variety of pathologic conditions.[2] A major morphologic correlate of retinal light damage is apoptotic cell death of photoreceptors and retinal pigment epithelium (RPE) cells.[3]

During apoptosis the immediate early gene and protooncogene *c-fos* is induced in several systems.[4,5] *c-fos* encodes the phosphoprotein c-Fos, a component of the nuclear transcription factor complex AP-1, which modulates the expression of a variety of genes also in the retina.[6–8] However, the physiological function of c-Fos in the retina remains to be investigated.

Under a regular dark–light cycle, retinal *c-fos* is expressed in a diurnal rhythm. *c-fos* is induced in the ganglion cell layer and in the inner nuclear layer after the onset of light but in the outer nuclear layer (ONL) during the dark period.[9–11]

Recently, it has been shown that *c-fos* plays an essential role in light-induced apoptosis of photoreceptors: after exposure to bright white light, wild-type mice (*c-fos*$^{+/+}$ mice) display severe loss of photoreceptor cells due to apoptosis, whereas retinas of mice without c-Fos (*c-fos*$^{-/-}$ mice) remain unaffected.[12] The observed resistance to light-induced apoptosis in *c-fos*$^{-/-}$ mice may indicate an active contribution of c-Fos to the apoptotic cascade triggered by light. Because c-Fos is suggested to play an important role in the regulation of rod-specific gene expression,[13] functional deficits in *c-fos*$^{-/-}$ mice may render their retinas insensitive to light. Finally, given the deficits in bone and cartilage development with reduced body weight,[14] it could be assumed that *c-fos*$^{-/-}$ mice are under constant stress. Stress may induce the expression of heat shock proteins that have been suggested to be involved in the resistance against light damage.[15]

To date, no information about functional properties of the retina in *c-fos*$^{-/-}$ mice is available. To elucidate the mechanism rendering *c-fos*$^{-/-}$ mice resistant to light-induced apoptosis,

From the [1]Neurophysiology, and [2]Retinal Cell Biology Laboratories, Department of Ophthalmology, University Hospital Zurich, Switzerland; and the [3]Department of Biology and Biochemistry, College of Optometry, University of Houston, Texas.

Supported by the Swiss National Science Foundation and Bruppacher Foundation, Zurich, Switzerland; E. and B. Grimmke Foundation, Düsseldorf, Germany (CG, FH, CER, and AW); and National Institutes of Health Grant ES-03183 (DAF).

Submitted for publication December 18, 1998; revised June 18 and August 16, 1999; accepted September 3, 1999.

Commercial relationships policy: N.

Corresponding author: Nicole Kueng–Hitz, Neurophysiology Laboratory, Department of Ophthalmology, University Hospital Zurich, Frauenklinikstrasse 24, CH-8091 Zurich, Switzerland.
nicole.kueng@aug.usz.ch

we compared the retina of *c-fos*$^{-/-}$ and *c-fos*$^{+/+}$ mice in their ability to absorb and transduce light. We studied retinal function by full-field electroretinograms (ERGs), and we compared retinal morphology by light and electron microscopy. We furthermore investigated critical components related to photoreception and phototransduction: the rhodopsin content and regeneration rate, the retinal photon absorption capacity, and the levels of arrestin, which deactivates rhodopsin.[16,17] To detect a possible candidate with protective potential against light damage, we furthermore determined the level of Hsp70.

METHODS

Transgenic Mice

All procedures concerning animals were conducted in accordance with the regulations of the Cantonal Veterinary Authority of Zurich and with the ARVO Statement for the Use of Animals in Ophthalmic and Vision Research. *c-fos*$^{+/+}$ and *c-fos*$^{-/-}$ mice were obtained from heterozygous matings (Jackson Laboratories, Bar Harbor, ME) on a C57BL/6x129Sv background. Only mice with equally pigmented eyes and dark brown coat color were used. *c-fos*$^{-/-}$ mice were phenotypically identified by the absence of teeth and smaller body size. For control, genotyping was performed by polymerase chain reaction in some instances. Mice were reared in a 12-hour dark-light cycle in 60 to 100 lux in the cages and analyzed at the age of 4 to 6 weeks.

Electroretinography

Sixteen male mice (eight *c-fos*$^{+/+}$, eight *c-fos*$^{-/-}$) were used for electroretinography, performed in a standardized timing and anesthesia protocol. After a 16-hour period of dark adaptation, mice underwent ERG recording. Body weight was measured before anesthesia, which was performed with a single intraperitoneal injection of xylazine (20 μg/g) and ketamine (40 μg/g). Mice were placed on a 38°C heating pad throughout the experimental session. After dilation of the pupils (Mydriaticum Dispersa; Ciba Vision, Niederwangen, Switzerland), full-field ERGs were recorded from the left eye using a silk Ag-AgCl electrode[18] placed centrally on the cornea. The reference electrode was placed in the mouth, and a needle electrode in the tail served as a ground. All manipulations were performed under very dim red light using an operating microscope. The position of the electrode was monitored with an infrared camera. White light stimuli of a halogen-source (model 150H; Volpi, Schlieren, Switzerland) of 20-msec duration were presented in order of increasing luminance over a range of 6 logarithmic units of intensity (8×10^{-2} to 8×10^{4} candela [cd]/m^2). Four consecutive responses were averaged with an interstimulus interval of 5 seconds for the a- and b-wave and with an interval of 7 seconds for the c-wave. Signals were digitized by a personal computer for off-line analysis[19] and written on a chart recorder (Kipp & Zonen; Recom Electronics, Horgen, Switzerland). The amplitude of the a-wave was measured from the prestimulus baseline to the trough of the a-wave. The amplitude of the b-wave was measured either from the trough of the a-wave to the positive peak or, at low intensities, from the baseline to the positive peak. Higher stimulus intensities evoked prominent oscillatory potentials that contributed to the amplitude of the b-wave. To obtain an unequivocal assessment of the time course of the b-wave, we therefore measured its latency from the time of the stimulus onset to the time of the beginning of the b-wave instead of measuring the implicit time. After the ERG recording, some of the mice were used for morphologic studies.

Morphology

Light microscopy was performed as described previously.[12] Briefly, eyes were enucleated and fixed in 2.5% glutaraldehyde in 0.1 M cacodylate buffer (pH 7.3) at 4°C overnight. For each eye, the superior and the inferior central retina adjacent to the optic nerve was trimmed, washed in cacodylate buffer, post-fixed in osmium tetroxide for 1 hour, dehydrated in increasing ethanol concentrations, and embedded in Epon 812. Sections (0.5 μm) were prepared from the superior and the inferior central retina, stained with methylene blue, and analyzed by microscopy (Axiophot; Zeiss, Oberkochen, Germany). For a comparison of rod outer segment (ROS) length, in every second of 10 photographs ($\times$740), each representing 125 μm, the distance from the ROS bases to the tips of the ROS layer adjacent to the RPE was determined.

For electron microscopy, eyes were removed and fixed by immersion fixation using 3% glutaraldehyde, 2% paraformaldehyde, and 0.1% $CaCl_2$ in 0.1M cacodylate buffer (pH 7.4). The tissue was embedded in Spurr's epoxy medium. Ultrathin sections were stained with 3.5% uranyl acetate and Reynold's lead citrate and examined using a transmission electron microscope (model 100-C; JEOL, Tokyo, Japan). Morphometry was performed on Spurr's embedded 1.2-μm sections stained with toluidine blue using a $\times$40 objective lens (total magnification, $\times$400) and a calibrated Filar micrometer eyepiece on a stereomicroscope (model BH-2; Olympus, Melville, NY). Counts of rod and cone photoreceptor nuclei were made at the posterior pole of the eye (central retina) and in the periphery of both the superior and the inferior temporal quadrants, as described earlier.[20] Twenty fields, each 100 μm in length, were examined in each of three sections from five *c-fos*$^{+/+}$ and four *c-fos*$^{-/-}$ mice: 10 beginning 100 μm from the optic nerve head and moving peripherally and another 10 beginning 100 μm from the ora serrata and moving posteriorly. The number of rod and cone photoreceptor cells was recorded in each region, and the mean was calculated for each animal. Then, the overall group mean, SEM, and percentage of each cell type were calculated.

Rhodopsin Content and Rhodopsin Regeneration

For the determination of the maximal rhodopsin contents mice were dark adapted for 16 hours. All subsequent manipulations were conducted under dim red light. Both retinas from one mouse were removed through a corneal slit and pooled in 1 ml ddH_2O. After centrifugation (15,000*g*, 3 minutes, 19°C) the supernatant was discarded, and retinas were resuspended in 0.7 ml 1% hexadecyltrimethyl-ammoniumbromide (Fluka Chemie, Buchs, Switzerland) in ddH_2O, homogenized with a polytron (20 seconds, 3000 rpm) and centrifuged as above.[21]The absorption at 500 nm of the resultant supernatant was measured in a spectrophotometer (Cary 50, Varian; Zug, Switzerland), using a plastic cuvette (path length, 1 cm). After exposing the sample to intense white light (20,000 lux) for 1 minute to bleach all present rhodopsin, the spectrophotometric measurement was repeated. The amount of rhodopsin present per retina was calculated using the following formula derived from the Lambert–Beer equation:

TABLE 1. Rhodopsin-Content in Retinas from *c-fos*$^{+/+}$ and *c-fos*$^{-/-}$ Mice Before and After Exposure to 5000 lux for 10 minutes

	c-fos$^{+/+}$	*c-fos*$^{-/-}$
Dark adapted	0.52 ± 0.05 (8)	0.39 ± 0.08 (5)
Minutes after light exposure		
0	0.03 ± 0.02 (5)	0.03 ± 0.00 (2)
5	0.05 (1)	n.d.
10	0.07 (1)	n.d.
15	0.07 ± 0.04 (3)	n.d.
30	0.13 (1)	0.15 ± 0.01 (2)
60	0.24 ± 0.1 (7)	0.14 ± 0.03 (3)
120	0.31 ± 0.08 (5)	n.d.
240	0.48 ± 0.06 (5)	0.38 ± 0.09 (3)

Data are mean nanomoles rhodopsin per eye ± SD with the number of retinas studied in parentheses.

$$rho = vol \times c = vol \times [\Delta abs_{500}/(e \times l \times n)]$$

where *rho* is the amount of rhodopsin per retina (in moles); *vol*, the volume of sample (in liters); *c*, the concentration of rhodopsin per retina (in mol/liters); Δ abs_{500} is the difference between absorption before and after bleaching measured at 500 nm; *e* is the extinction coefficient of rhodopsin at 500 nm (4.2×10^4 cm × M); *l* is the path length of the plastic cuvette (in centimeters); and *n* is the number of retinas.

To assess the regeneration kinetics of rhodopsin in vivo, pupils of animals were dilated under dim red light (Cyclogyl 1%; Alcon, Cham, Switzerland; and phenylephrine 5%, Ciba Vision, Niederwangen, Switzerland) after 16 hours of dark adaptation, and animals were exposed to 5000 lux diffuse white fluorescent light (TLD-36 tubes; Philips, Hamburg, Germany; UV-impermeable diffuser) in cages with a reflective interior for 10 minutes. Rhodopsin content was determined immediately (0 minutes, nearly complete bleaching) or after 5, 10, 15, 30, 60, 120, and 240 minutes (*c-fos*$^{+/+}$) and 0, 30, 60, and 240 minutes (*c-fos*$^{-/-}$) in darkness, as described. Using those values for rhodopsin per retina (Table 1), the resultant regeneration constants and the number of photons absorbed per 10 minutes by mice of both genotypes were calculated for the steady state of bleaching, as described by Penn and Williams.[22]

Arrestin- and Hsp70 Western Blot Analysis

Three mice of each genotype were used for Western blot analysis. Retinas from dark-adapted mice (16 hours), were transferred into 200 μl ice-cold phosphate-buffered saline, homogenized using an ultrasound tip, and analyzed for their protein content using the Bradford method (BioRad, Richmond, CA) with a bovine serum albumin standard. Sixty-seven μl 4× sodium dodecyl sulfate–polyacrylamide gel electrophoresis (SDS-PAGE) sample buffer was added to the homogenates, and samples were heated for 10 minutes at 70°C. SDS-PAGE (7.5%) and Western blot analysis were performed as described earlier.[23] For immunodetection, polyclonal rabbit antisera directed against arrestin (gift from Theo van Veen, University of Göteborg, Sweden)[24] and Hsp70 (Hsc70 and Hsp70 reactive, gift from A. Patrick Arrigo, University Claude Bernard, Lyon, France)[25] were applied. Horseradish peroxidase–conjugated secondary antibody was purchased from Santa Cruz Biotechnology (catalog no. SC2004; Santa Cruz, CA). Immunoreactivity was visualized using the enhanced chemiluminescence system (Amersham, Buckinghamshire, UK).

RESULTS

Electroretinography

The analysis of the ERG recordings revealed comparable and normal configurations of the a- and b-waves (Fig. 1A) as well as of the c-waves (Fig. 1B) for both *c-fos*$^{+/+}$ and *c-fos*$^{-/-}$ mice. Similarly, oscillatory potentials occurred at 8×10^2 to 8×10^3 cd/m^2 in both genotypes (Fig. 1A).

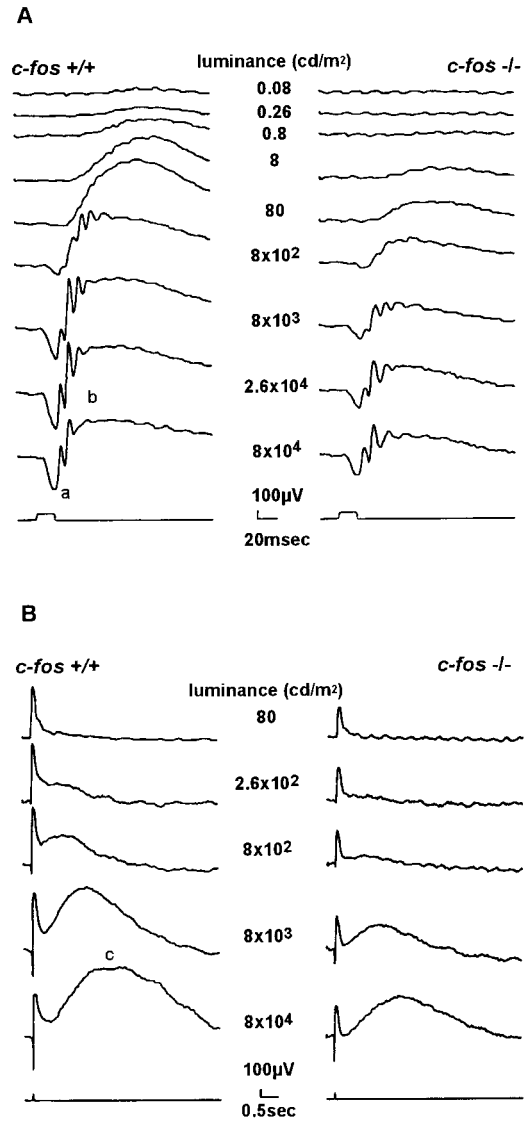

FIGURE 1. Original ERG-traces of an intensity series from dark-adapted *c-fos*$^{+/+}$ mice (*left column*) and *c-fos*$^{-/-}$ mice (*right column*). For clarity, a-, b-, and c-waves are marked. (**A**) a-Waves and b-waves with oscillatory potentials; bandpass, 0.3 to 500 Hz (average of $n = 4$). The *lowermost trace* represents a light stimulus of 20 msec. (**B**) c-Waves; bandpass, 0.03 to 500 Hz (average of $n = 4$). The *lowermost trace* represents the light stimulus of 200 msec. Note that the b-waves are not fully presented because of the limited A/D resolution at this time base that resolves the c-waves best.

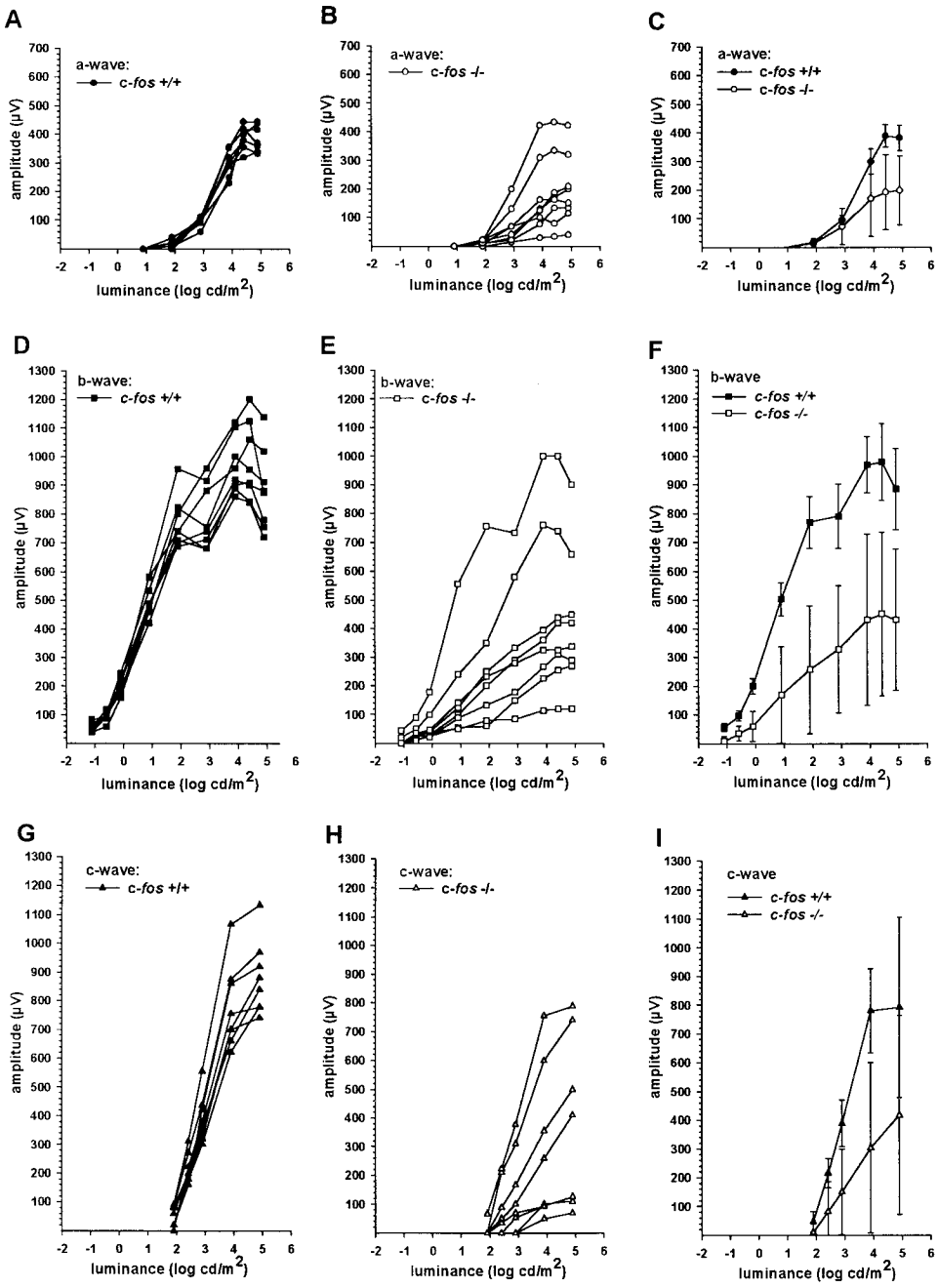

FIGURE 2. Curves of the luminance–response functions of *c-fos*$^{+/+}$ (*filled symbols*) compared with *c-fos*$^{-/-}$ mice (*open symbols*). (**A**, **B**, **C**) a-Waves, (**D**, **E**, **F**) b-waves, and (**G**, **H**, **I**) c-waves. The *left column* (**A**, **D**, **G**) shows the individual curves of the luminance–response functions of *c-fos*$^{+/+}$ mice. The *middle column* (**B**, **E**, **H**) shows the individual curves of the luminance–response functions of *c-fos*$^{-/-}$ mice. The *right column* (**C**, **F**, **I**) compares the mean values between both groups. Bars, SD.

In *c-fos*$^{+/+}$ mice the curves of the luminance–response functions of the a-, b-, and c-waves were highly reproducible (Figs. 2A, 2D, 2G), whereas *c-fos*$^{-/-}$ mice showed a large variability (Figs. 2B, 2E, 2H) with markedly lower mean values (Figs. 2C, 2F, 2I). In addition, the curves of the luminance–response functions of the a- and b-waves of *c-fos*$^{-/-}$ mice showed a shift to the right, indicating reduced retinal sensitivity. From the mean values of the b-waves, this shift was assessed to 0.9 log units. This value was obtained not only by assessing the luminance required to generate a one-half maximal b-wave, but also by comparing the luminance required to evoke a 100-μV criterion response, which might be taken as an extrapolated measure for rod sensitivity. The observed shift of the luminance–response functions of the a-waves was 0.2 log units, which was assessed by comparing the mean values of the luminances required to generate a 50-μV criterion response.

Compared with those in *c-fos*$^{+/+}$ mice, the mean values of the latencies of the b-waves were higher in *c-fos*$^{-/-}$ mice, and at higher luminances, this difference tended to disappear (Fig. 3). The time course revealed more variability in *c-fos*$^{-/-}$ mice, as indicated by the larger SDs.

Morphology

The ONL of retinas of both genotypes showed a distinctive chromatin pattern for rod and cone nuclei (Fig. 4). The ONL of *c-fos*$^{+/+}$ mice was found to be 10 to 11 rod nuclei thick, and rods comprised approximately 96% of the total photoreceptor population (Table 2). No differences were detected in the

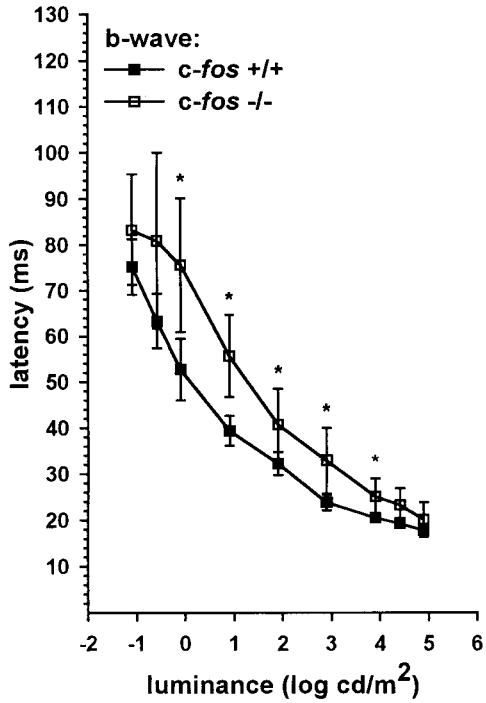

FIGURE 3. Latencies of the b-waves of *c-fos*$^{+/+}$ (*filled symbols*) and *c-fos*$^{-/-}$ mice (*open symbols*). Each *square* indicates the mean value of eight mice, except the two lowest luminances of the *c-fos*$^{-/-}$ mice ($n = 3$ at -1.5 log cd/m^2; $n = 7$ at -0.6 log cd/m^2). Bars, SD. *Asterisks* indicate a significant difference (from the lowest to the highest luminance: $P = 0.27$, 0.054, 0.006, 0.003, 0.0207, 0.003, 0.003, 0.015, and 0.13, respectively; Mann–Whitney). The increasing variability with decreasing luminances in both genotypes can be explained by the difficulty in assessing the latencies at very low luminances.

number of rod or cone cells in the superior compared with the inferior retina. The number of rod cells declined from the posterior pole of the retina (126 rods per 100 μm) to the periphery (103 rods per 100 μm), similar to the results of Carter-Dawson et al.[26] in C57BL/6J mice. In contrast, in *c-fos*$^{-/-}$ mice, the ONL was decreased in thickness (9–10 rod nuclei thick) in the superior and the inferior hemisphere and in the central and peripheral retina. This resulted in an overall decrease of 22% to 24% in the number of rods. The number of cones, however, was unaffected (Table 2).

In both genotypes, the length of ROS in the superior and inferior central retina, the region most susceptible to light damage, was comparable (superior, 27 ± 1 μm in *c-fos*$^{+/+}$ and 27 ± 2 μm in *c-fos*$^{-/-}$ mice; means ± SD, $n = 4$ and $n = 5$, respectively; inferior, 28 ± 5 μm in *c-fos*$^{+/+}$ and 27 ± 3 μm in *c-fos*$^{-/-}$ mice; means ± SD, $n = 4$ and $n = 5$, respectively).

Rhodopsin Content and Rhodopsin Regeneration: Number of Photons Absorbed

A significant reduction of 25% in rhodopsin content was found in *c-fos*$^{-/-}$ mice (Table 1, $P < 0.001$, two-way analysis of variance) when compared with *c-fos*$^{+/+}$ mice. Almost complete bleaching was achieved in dark-adapted animals within 10 minutes of exposure to 5000 lux (*c-fos*$^{+/+}$, 94% bleached; *c-fos*$^{-/-}$, 92% bleached). Bleached rhodopsin was nearly entirely regenerated during 240 minutes in darkness (*c-fos*$^{+/+}$, 92%; *c-fos*$^{-/-}$, 98%).

The regeneration rates for rhodopsin calculated from the values displayed in Table 1 were 0.01 per minute for *c-fos*$^{+/+}$ and 0.016 per minute for *c-fos*$^{-/-}$, indicating a slightly faster regeneration in *c-fos*$^{-/-}$ mice. Because the calculation of the number of photons absorbed[22] is only appropriate if bleaching versus regeneration is in a steady state, rhodopsin levels during bleaching were determined for wild-type mice at 10 minutes, 30 minutes, and 60 minutes. No difference in rhodopsin levels per retina was observed among the three time points (10 minutes, 0.03 nanomoles; 30 minutes, 0.03 nanomoles; 60 minutes, 0.04 nanomoles; $n = 3$ for 30 and 60 minutes; not

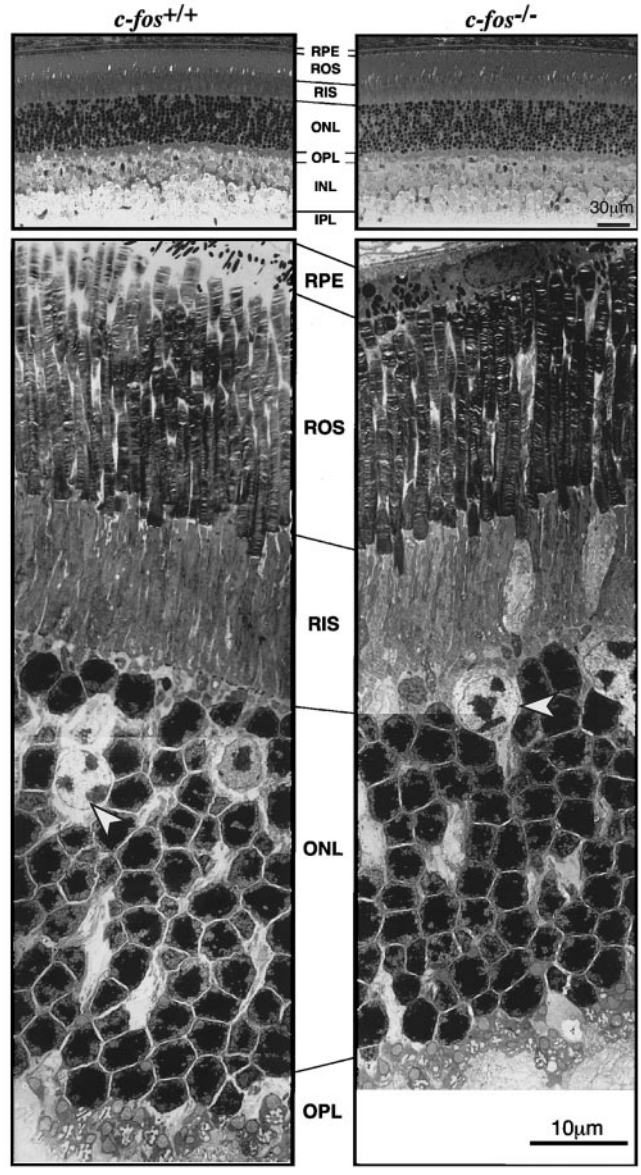

FIGURE 4. *Top*: Light micrographs from the inferior central part of the retina of *c-fos*$^{+/+}$ and *c-fos*$^{-/-}$ mice. Both genotypes show grossly comparable morphology. *Bottom*: Montages of electronmicrographs of the photoreceptor layer of *c-fos*$^{+/+}$ and *c-fos*$^{-/-}$ mice. Photoreceptor nuclei appear densely packed, and ROS and rod inner segments (RIS) display regular morphologic features in both genotypes. The *arrowheads* indicate cones. RPE, retinal pigment epithelium; OPL, outer plexiform layer; INL, inner nuclear layer; IPL, inner plexiform layer. Original magnification: *Top*, ×500; *bottom*, ×2240.

TABLE 2. Rod and Cone Nuclei in Sections of Superior and Inferior Temporal Retina from Adult *c-fos*–Deficient Mice (*c-fos*$^{-/-}$) and Littermate Control Animals (*c-fos*$^{+/+}$)

	c-fos$^{+/+}$			*c-fos*$^{-/-}$		
	Superior	**Inferior**	**Percent Remaining**	**Superior**	**Inferior**	**Percent Remaining**
Posterior (central) retina						
Rod nuclei	123.9 ± 2.9	127.2 ± 3.3	100 ± 3	93.6 ± 2.3*	97.2 ± 1.5*	76 ± 4
Cone nuclei	3.9 ± 0.2	3.8 ± 0.1	100 ± 3	3.9 ± 0.2	4.1 ± 0.2	104 ± 4
Peripheral retina						
Rod nuclei	103.9 ± 3.1	101.7 ± 2.4	100 ± 3	79.4 ± 2.0*	81.8 ± 1.6*	78 ± 3
Cone nuclei	3.8 ± 0.2	3.7 ± 0.2	100 ± 2	3.8 ± 0.2	4.0 ± 0.1	104 ± 4

The rod and cone counts are based on twenty 100-μm lengths; 10 consecutive lengths in each of three sections from five *c-fos*$^{+/+}$ and four *c-fos*$^{-/-}$ retinas.

*Significantly different from *c-fos*$^{+/+}$ at $P < 0.05$.

shown), indicating that the steady state is reached at 10 minutes and exists for at least 60 minutes.

The calculation of the number of photons absorbed at steady state gave the following results: *c-fos*$^{+/+}$ mice absorbed 2.9×10^{13} photons and *c-fos*$^{-/-}$ absorbed 3.4×10^{13} photons per retina per 10 minutes of exposure to 5000 lux.

Immunodetection of Arrestin and Hsp70

A very slight reduction in arrestin levels was detected in extracts from *c-fos*$^{-/-}$ mice, judged by comparing band staining intensities on Western blot analysis between *c-fos*$^{+/+}$ and *c-fos*$^{-/-}$ mice (Fig. 5). The Hsp70-antiserum detected comparable amounts of the constitutive form of Hsp70 (Hsc70, 73 kDa) in extracts of both genotypes. After prolonged exposure of the x-ray film, a faint band corresponding to the inducible form of Hsp70 (Hsp70, 72 kDa) became visible. No apparent difference was observed between *c-fos*$^{+/+}$ and *c-fos*$^{-/-}$ mice (Fig. 5).

DISCUSSION

Two major differences between *c-fos*$^{+/+}$ and *c-fos*$^{-/-}$ mice emerge from the present study: First, retinas of *c-fos*$^{-/-}$ mice show a marked and variable attenuation of their functional properties, resulting in lower ERG-amplitudes and a 0.9-log-unit lower b-wave sensitivity. Second, they have 22% to 24% less rods and 25% less rhodopsin. However, retinas of both genotypes display comparable photon absorption rates at 5000 lux, the intensity used to induce light damage.[12]

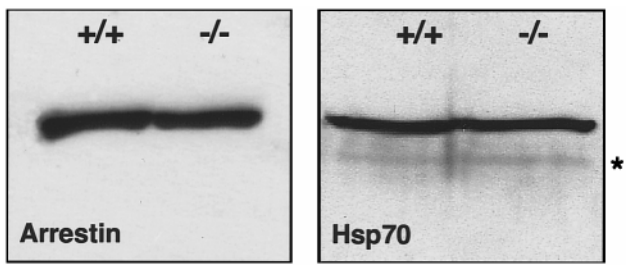

FIGURE 5. Immunodetection of arrestin and Hsp70 by Western blot analysis prepared from total retinal homogenates (10 μg protein for arrestin, 25 μg protein for Hsp70) of *c-fos*$^{+/+}$ and *c-fos*$^{-/-}$ mice. The Hsp70 antiserum detected the constitutive form of Hsp70 (Hsc70, 73 kDa) and the inducible form of Hsp70 (Hsp70, 72 kDa, faint band, indicated with *asterisk*).

Variability in *c-fos*$^{-/-}$ Mice

c-fos$^{-/-}$ mice display a remarkable variability of all electrophysiological data. Similarly, we observed a larger variability in body weight of age-matched *c-fos*$^{-/-}$ mice than in wild-type mice (±35.3% SD in *c-fos*$^{-/-}$ mice, ±19.9% SD in *c-fos*$^{+/+}$ mice; $n = 8$ each). The lower variability observed in *c-fos*$^{+/+}$ mice grown on an identical genetic background, indicates a higher sensitivity to epigenetic influences in *c-fos*$^{-/-}$ mice. These observations of phenotypic heterogeneity complement the results of behavioral tests in these mice.[27]

Electroretinography

The normal configuration of the full-field ERG-recordings of *c-fos*$^{+/+}$ and *c-fos*$^{-/-}$ mice demonstrates photoreceptor activity (a-wave), inner retinal activity (b-wave and oscillatory potentials), and a functional photoreceptor-RPE interaction (c-wave). These results indicate that *c-fos* is not essential for the ability to absorb photons, for phototransduction or for the function of second-order neurons. It is evident, however, that retinal function in *c-fos*$^{-/-}$ mice is attenuated markedly, resulting in lower mean amplitudes, longer mean latencies, and reduced retinal sensitivity. This attenuation in retinal sensitivity in *c-fos*$^{-/-}$ mice amounts to 0.2 log units for the a-wave and to 0.9 log units for the b-wave, indicating a larger postreceptoral functional difference between *c-fos*$^{+/+}$ and *c-fos*$^{-/-}$ mice. At higher luminances the mean latencies in the two genotypes differed less than at lower luminances. Based on pure rod responses at lower luminances but an increasing contribution of the cone system at higher luminances, the functional differences between both genotypes therefore may affect the rod system rather than the cone system. This suggestion would correspond to a reduced number of rods, a lower rhodopsin content, and an unaltered number of cones observed in *c-fos*$^{-/-}$ mice.

Morphology

c-fos$^{-/-}$ mice display a selective reduction of rod photoreceptors with no preference for any retinal area. This reduction may occur because of a reduced differentiation of precursor cells into rods or because of increased developmental apoptosis. However, because of a grossly unaltered morphology, it ap-

pears that developmental apoptosis in the retina proceeds normally in the absence of *c-fos*, suggesting that other proteins of the AP-1 family can substitute for the absence of *c-fos* during development. Our observation thus complements an earlier report.[28]

Rhodopsin Content and Regeneration

The values of rhodopsin determined after 16 hours of dark adaptation are likely to reflect maximal values in *c-fos*$^{+/+}$ and *c-fos*$^{-/-}$ mice, because both types of mice almost completely regenerated rhodopsin within 4 hours after bleaching. The rhodopsin content in *c-fos*$^{-/-}$ mice was reduced by 25% in dark adaptation. Because a shortening of ROS, at least in central areas, was not observed, it appears likely that this reduction is based solely on the absence of 22% to 24% rods in these animals. Thus, at the level of single cells, the individual rod in *c-fos*$^{-/-}$ mice is most likely furnished with the same amount of rhodopsin as is its wild-type counterpart.

Arrestin

Activated rhodopsin may stimulate the phototransduction cascade differently in *c-fos*$^{+/+}$ compared with *c-fos*$^{-/-}$ mice, for example, because of deviant deactivation kinetics. The deactivation of rhodopsin depends on arrestin,[16] and increased levels of arrestin in ROS have been associated with reduced retinal sensitivity.[29] Arrestin is exclusively expressed in photoreceptors. Accordingly, a reduction of arrestin immunoreactivity might be expected in extracts from *c-fos*$^{-/-}$ mice corresponding to the loss of 23% rods. However, as judged by visual impression, the reduction of band staining for arrestin on Western blots of *c-fos*$^{-/-}$ retinal extracts appeared less prominent. Thus, rods of *c-fos*$^{-/-}$ mice may contain slightly elevated arrestin levels and therefore have an increased ratio of arrestin to rhodopsin. This, however may not influence the deactivation of rhodopsin: Studies in transgenic mice indicate that binding of arrestin to photoisomerized rhodopsin is not rate-limiting in quenching the activity of rhodopsin.[17]

Relations between Functional Parameters, Rhodopsin Content, and Morphology

Several reports demonstrate that changes in rhodopsin content are accompanied by functional and morphologic deficits of photoreceptor cells.[30–33] Changes in rhodopsin content due to an increased background intensity, after bleaching, or under vitamin A deficiency have been shown to raise threshold for ERG criterion responses in a systematic manner.[34–36] In correspondence, attenuated retinal function in *c-fos*$^{-/-}$ mice in our study was associated with a lower rhodopsin content and with a reduction in the number of rods.

Whether this attenuation is primarily caused by the reduction in the number of rods and/or rhodopsin or whether components of the phototransduction cascade other than rhodopsin are also differently expressed in *c-fos*$^{-/-}$ mice remains to be investigated. It appears also conceivable that postreceptoral processes contribute to the differences in retinal function in *c-fos*$^{+/+}$ and *c-fos*$^{-/-}$ mice.

Resistance to Light Damage in *c-fos*$^{-/-}$ Mice

The susceptibility to light damage is determined by several factors[37,38] and may be reduced by protective mechanisms such as upregulated heat shock proteins.[15]

We determined the levels of Hsc70 and Hsp70, which are members of the Hsp70 family. Both show antiapoptotic properties,[39–41] and particularly Hsp70 has been suggested to be involved in the resistance against light damage.[15] Assuming that in mice Hsp70 is primarily expressed in the ONL, as is the case in rats,[42] a reduction of the inducible form of Hsp70 in *c-fos*$^{-/-}$ mice might be expected, corresponding to the loss of 23% of the rods. Thus, similar levels of Hsp70 in extracts from retinas of *c-fos*$^{+/+}$ and *c-fos*$^{-/-}$ mice may suggest that it is elevated in the remaining rods of *c-fos*$^{-/-}$ mice. Nevertheless, it appears unlikely that a maximum increase of 23% accounts for the complete protection of rods against light-induced apoptosis. In this regard, a 20% increased expression of Hsp70 did not confer resistance against various apoptotic stimuli in cultured murine fibrosarcoma cells, whereas five- to sixfold elevated Hsp70 levels made these cells resistant.[41]

c-fos$^{-/-}$ mice showed attenuated but normally configured ERGs. It is not clear whether or to what extent this attenuation influences the susceptibility to light damage.

Although light damage may be rhodopsin mediated,[43] it appears unlikely that the resistance to light-induced damage in *c-fos*$^{-/-}$ mice depends exclusively on a 25% reduced rhodopsin content. This assumption is supported by the following observations: First, the maximal rhodopsin value found in *c-fos*$^{-/-}$ (0.45 nanomoles) exceeds the lowest value found in *c-fos*$^{+/+}$ mice (0.41 nanomoles). However, all *c-fos*$^{+/+}$ mice tested in our laboratory so far ($n > 50$) showed light damage, but *c-fos*$^{-/-}$ mice never did ($n > 30$). Second, the calculation of the number of photons absorbed per retina per time, revealed comparable abilities to absorb photons at 5000 lux, perhaps because of the slightly faster regeneration of rhodopsin and despite its decreased dark-adapted levels in *c-fos*$^{-/-}$ mice. Interestingly, 50 minutes of exposure to this intensity are sufficient to induce light damage in *c-fos*$^{+/+}$ mice (Wenzel A, Remé CE, Williams TP, Hafezi F, Grimm C, unpublished data, January–March, 1998). Furthermore, because the retina of *c-fos*$^{-/-}$ mice contains less rods, its individual rod may absorb even more photons during this time than a rod of a *c-fos*$^{+/+}$ mouse. However, rods of *c-fos*$^{-/-}$ mice are protected against light-induced apoptosis, indicating that the signaling cascade leading from bleaching of rhodopsin to the induction of apoptosis is interrupted downstream of rhodopsin because of the absence of *c-fos*.

Acknowledgments

The authors thank Theodore P. Williams, Florida State University, Tallahassee, for advice on calculating photon absorption; Fabio Valeri, University Hospital Zurich, Switzerland, for advice on statistics; and Kurt Munz for skilled technical assistance.

References

1. Young RW. Cell death during differentiation of the retina in the mouse. *J Comp Neurol.* 1984;229:362–373.
2. Remé CE, Grimm C, Hafezi F, Marti A, Wenzel A. Apoptotic cell death in retinal degenerations. In: Osborne NN, Chader GJ, eds. *Progress in Retinal and Eye Research.* Oxford: Elsevier Science; 1998:443–464.
3. Hafezi F, Marti A, Munz K, Remé CE. Light-induced apoptosis: differential timing in the retina and pigment epithelium. *Exp Eye Res.* 1997;64:963–970.
4. Smeyne RJ, Vendrell M, Hayward M, et al. Continuous c-fos expression precedes programmed cell death in vivo. *Nature.* 1993; 363:166–169.

5. Estus S, Zaks WJ, Freeman RS, et al. Altered gene expression in neurons during programmed cell death: identification of c-jun as necessary for neuronal apoptosis. *J Cell Biol.* 1994;127:1717–1727.
6. Kumar R, Chen S, Scheurer D, et al. The bZIP transcription factor Nrl stimulates rhodopsin promotor activity in primary retinal cell cultures. *J Biol Chem.* 1996;271:29612–29618.
7. Di Polo A, Lerner LE, Farber DB. Isolation and initial characterization of the 5′ flanking region of the human and murine cyclic guanosine monophosphate-phosphodiesterase beta-subunit genes. *Nucleic Acids Res.* 1997;25:3863–3867.
8. Tao L, Pandey S, Simon MI, Fong HK. Structure of the bovine transducin gamma subunit gene and analysis of promoter function in transgenic mice. *Exp Eye Res.* 1993;56:497–507.
9. Nir I, Agarwal N. Diurnal expression of c-fos in the mouse retina. *Brain Res.* 1993;19:47–54.
10. Harada T, Imaki J, Ohki K, et al. Cone-associated *c-fos* gene expression in the light-damaged rat retina. *Invest Ophthalmol Vis Sci.* 1996;37:1250–1255.
11. Yoshida K, Kawamura K, Imaki J. Differential expression of c-fos RNA in rat retinal cells: regulation by light/dark cycle. *Neuron.* 1993;10:1049–1054.
12. Hafezi F, Steinbach JP, Marti A, et al. The absence of c-fos prevents light-induced apoptotic cell death of photoreceptors in retinal degeneration in vivo. *Nat Med.* 1997;3:346–349.
13. He L, Campbell ML, Srivastava D, et al. Spatial and temporal expression of AP-1 responsive rod photoreceptor genes and bZIP transcription factors during development of the rat retina. *Mol Vis.* 1998;4:32 available at http://www.molvis.org/molvis/v4/p32
14. Wang ZQ, Ovitt C, Grigoriadis E, et al. Bone and haematopoietic defects in mice lacking *c-fos. Nature.* 1992;360:741–745.
15. Barbe MF, Tytell M, Gower DJ, Welch WJ. Hyperthermia protects against light damage in the rat retina. *Science.* 1988;241:1817–1820.
16. Wilden U, Hall SW, Kuhn H. Phosphodiesterase activation by photoexcited rhodopsin is quenched when rhodopsin is phosphorylated and binds the intrinsic 48-kDa protein of rod outer segments. *Proc Natl Acad Sci USA.* 1986;83:1174–1178.
17. Xu J, Dodd RL, Makino CL, et al. Prolonged photoresponses in transgenic mouse rods lacking arrestin. *Nature.* 1997;389:505–509.
18. Niemeyer G, Kueng N. A simple and stable d.c. electrode for ocular electrophysiology. *Doc Ophthalmol.* 1999;95:55–61.
19. Kaelin–Lang A, Niemeyer G, Ein PC. Programm für die Auswertung elektrophysiologischer Signale vom Säugetierauge. *Klin Monatsbl Augenheilkd.* 1995;206:394–396.
20. Fox DA, Chu LW. Rods are selectively altered by lead, II: ultrastructure and quantitative histology. *Exp Eye Res.* 1988;46:613–625.
21. Baker BN, Breil SJ, Williams TP. Flash bleaching of rhodopsin in cetyltrimethylammonium bromide. *Vision Res.* 1972;12:1785–1794.
22. Penn JS, Williams TP. Photostasis: regulation of daily photon-catch by rat retinas in response to various cyclic illuminances. *Exp Eye Res.* 1986;43:915–928.
23. Wenzel A, Benke D, Mohler H, Fritschy JM. N-methyl-D-aspartate receptors containing the NR2D subunit in the retina are selectively expressed in the rod bipolar cells. *Neuroscience.* 1997;78:1105–1112.
24. Long K, Philp N, Gery I, Aguirre G. S-antigen in a hereditary visual cell disease: immunocytochemical and immunological studies. *Invest Ophthalmol Vis Sci.* 1988;29:1594–1607.
25. Mehlen P, Preville X, Chareyron P, et al. Constitutive expression of human hsp27, Drosophila hsp27, or human alpha B-crystallin confers resistance to TNF- and oxidative stress-induced cytotoxicity in stably transfected murine L929 fibroblasts. *J Immunol.* 1995;154:363–374.
26. Carter–Dawson RD, La Vail MM, Sidman RL. Differential effect of the rd mutation on rods and cones in the mouse retina. *Invest Ophthalmol Vis Sci.* 1978;17:489–498.
27. Paylor R, Johnson RS, Papaioannou VE, Spiegelman BM, Wehner JM. Behavioral assessment of c-*fos* mutant mice. *Brain Res.* 1994;651:257–282.
28. Roffler–Tarlov S, Brown JJG, Tarlov E, et al. Programmed cell death in the absence of c-Fos and c-Jun. *Development.* 1996;122:1–9.
29. Williams MA, Mangini NJ. Immunolocalization of arrestin (S-antigen) in rods of pearl mutant and wild-type mice. *Curr Eye Res.* 1991;10:457–462.
30. Bonting SL, Caravaggio LL, Gouras P. The rhodopsin cycle in the developing rat, I: relation of rhodopsin content, electroretinogram and rod structure in the rat. *Exp Eye Res.* 1961;1:14–24.
31. Smith SB, Hamasaki DI. Electroretinographic study of the C57BL/6-mi^{vit}/mi^{vit} mouse model of retinal degeneration. *Invest Ophthalmol Vis Sci.* 1994;35:3119–3123.
32. Fox DA, Rubinstein SD. Age-related changes in retinal sensitivity, Rhodopsin content and rod outer segment length in hooded rats following low-level lead exposure during development. *Exp Eye Res.* 1989;48:237–249.
33. Fox DA, Campbell ML, Blocker YS. Functional alterations and apoptotic cell death in the retina following developmental or adult lead exposure. *Neurotoxicology.* 1997;18:645–664.
34. Fain G, Lisman JE. Photoreceptor degeneration in vitamin A deprivation and retinitis pigmentosa: the equivalent light hypothesis. *Exp Eye Res.* 1993;57:335–340.
35. Dowling JE, Ripps H. Visual adaptation in the retina of the skate. *J Gen Physiol.* 1970;56:491–520.
36. Perlman I. Kinetics of bleaching and regeneration of rhodopsin in abnormal (RCS) and normal albino rats in vivo. *J Physiol (Lond).* 1978;278:141–159.
37. Organisciak DT, Winkler BS. Retinal light damage: practical and theoretical considerations. In: Osborne NN, Chader GJ, eds. *Progress in Retinal and Eye Research.* Oxford: Pergamon Press; 1994:1–29.
38. Remé ChE, Hafezi F, Marti A, Munz K, Reinboth JJ. Light damage to retina and pigment epithelium. In: Marmor MF, Wolfensberger TJ, eds. *The Retinal Pigment Epithelium: Function and Disease.* New York: Oxford University Press; 1998:563–586.
39. Takayama S, Bimston DN, Matsuzawa S, et al. BAG-1 modulates the chaperone activity of Hsp70/Hsc70. *EMBO J.* 1997;16:4887–4896.
40. Hohfeld J. Regulation of the heat shock conjugate Hsc70 in the mammalian cell: the characterization of the anti-apoptotic protein BAG-1 provides novel insights. *Biol Chem.* 1998;379:269–274.
41. Jaattela M, Wissing D, Kokholm K, Kallunki T, Egeblad M. Hsp70 exerts its anti-apoptotic function downstream of caspase-3-like proteases. *EMBO J.* 1998;17:6124–6134.
42. Dean DO, Kent CR, Tytell M. Constitutive and inducible heat shock protein 70 immunoreactivity in the normal rat eye. *Invest Opthalmol Vis Sci.* 1999;40:2952–2962.
43. Noell WK. There are different kinds of retinal light damage in the rat. In: Williams TP, Baker BN, eds. *The Effects of Constant Light on Visual Processes.* New York: Plenum Press; 1980:3–28.